

# AGB AND POST-AGB EVOLUTION: STRUCTURAL AND CHEMICAL CHANGES

T. Blöcker, R. Osterbart, G. Weigelt

*Max-Planck-Institut für Radioastronomie, 53121 Bonn, Germany*

Y. Balega

*Special Astrophysical Observatory, Nizhnij Arkhyz, 357147, Russia*

A. Men'shchikov

*Stockholm Observatory, 13336 Saltsjöbaden, Sweden*

**Abstract** Structural and chemical changes during the AGB and post-AGB evolution are discussed with respect to two recent observational and theoretical findings. On the one hand, high-resolution infrared observations revealed details of the dynamical evolution of the fragmented, bipolar dust shell around the far-evolved carbon star IRC +10 216 giving evidence for rapid changes of an already PPN-like structure during the very end of the AGB evolution. On the other hand, stellar evolution calculations considering convective overshoot have shown how thermal pulses during the post-AGB stage lead to the formation of hydrogen-deficient post-AGB stars with abundance patterns consistent with those observed for Wolf-Rayet central stars.

## 1. INTRODUCTION

During the evolution along the Asymptotic Giant Branch (AGB) and the subsequent post-AGB phases various structural and chemical changes of the stars and their surrounding dust-shells and nebulae take place. One important issue is the change of the dust-shell symmetry during transition from the AGB to the post-AGB stage. Unlike dust-shells around AGB stars, post-AGB objects as protoplanetary nebulae often expose prominent features of asphericities, in particular in axisymmetric geometry (e.g. Olofsson 1996). The shaping of planetary nebulae can be described by interacting stellar wind theories (see Kwok 2000) treating the interaction of a fast (spherical) central-star wind with the preceding slow (aspherical) AGB wind. The establishment of bipo-

lar structures seems to begin already during the (very end of) AGB evolution. One example of this stage of evolution is the carbon star IRC+10216. Its recent high-resolution observations indicate asymmetric mass-loss processes and even give insight into its dynamical dust-shell evolution (Osterbart et al. 2000).

Another matter of debate is the origin of hydrogen-deficient post-AGB stars. Although stars evolving through the AGB phase stay hydrogen-rich at their surfaces, a considerable fraction of their descendants, the central stars of planetary nebulae (CSPNe), show hydrogen-deficient compositions (Mendez 1991). Approximately 20% of the whole CSPNe population appears to be hydrogen deficient while the rest show solar-like compositions. Important constituents of the hydrogen-deficient population are the Wolf-Rayet (WR) central stars and the hot PG 1159 stars with typical surface abundances of (He,C,O)=(33,50,17) by mass (Dreizler & Heber 1998, Koesterke & Hamann 1997). Standard stellar evolution calculations failed to model these objects since they predict post-AGB stars either to have hydrogen-rich surfaces (e.g. Blöcker 1995) or, if hydrogen-deficient, to expose only a few percent of oxygen in their photospheres (Iben & McDonald 1995). However, if convective overshoot is considered, hydrogen-deficient post-AGB stars with abundance patterns as observed in WR central stars can be formed (Blöcker 2000, Herwig 2000).

## 2. THE DUST-SHELL OF IRC+10216

IRC+10216 (CW Leo) is the nearest ( $d \sim 130$  pc, Groenewegen 1997) and best-studied carbon star and one of the brightest infrared sources in the sky. Due to strong stellar winds of  $\dot{M} \approx 2 - 5 \times 10^{-5} M_{\odot} \text{ yr}^{-1}$  (Loup et al. 1993) it is highly enshrouded by dust. The central star of IRC+10216 is a long-period variable with a period of  $\sim 649$  days (Le Bertre 1992). The bipolar appearance of the dust shell around this object was reported by Kastner & Weintraub (1994). The non-spherical structure is consistent with the conjecture that IRC+10216 is in a phase immediately before entering the protoplanetary nebula stage. High-resolution observations showed that the inner circumstellar dust shell is fragmented (Weigelt et al. 1998, Haniff & Buscher 1998). The results of Dyck et al. (1991) and Haniff & Buscher (1998) showed that the dust-shell structure of IRC+10216 is changing within a timescale of only several years. The dynamical dust-shell evolution was revealed in detail by recent observations of Osterbart et al. (2000) and Tuthill et al. (2000).

Figures 1-2 show  $J$ -,  $H$ -, and  $K$ -band observations of IRC+10216 (Osterbart et al. 2000). The images were reconstructed from 6 m telescope speckle interferograms using the bispectrum speckle interferometry method (Weigelt 1977, Lohmann et al. 1983, Weigelt 1991). The  $H$  and  $K$  images with resolutions between 70 mas and 92 mas consist of several compact components within a 0.2'' radius and a fainter asymmetric nebula. A series of  $K$ -band im-

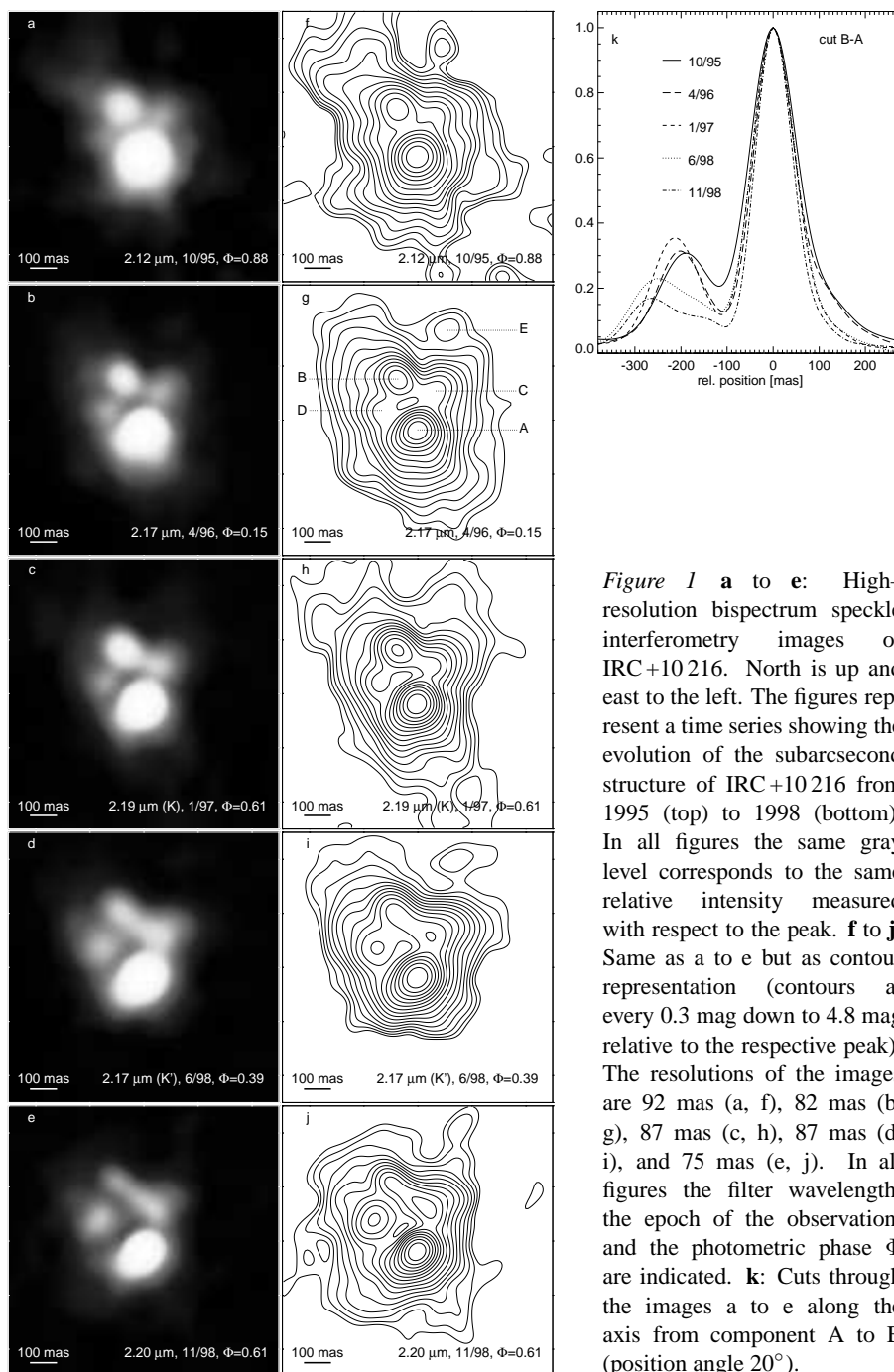


*Figure 1 a to e:* High-resolution bispectrum speckle interferometry images of IRC+10216. North is up and east to the left. The figures represent a time series showing the evolution of the subarcsecond structure of IRC+10216 from 1995 (top) to 1998 (bottom). In all figures the same gray level corresponds to the same relative intensity measured with respect to the peak. **f to j:** Same as a to e but as contour representation (contours at every 0.3 mag down to 4.8 mag relative to the respective peak). The resolutions of the images are 92 mas (a, f), 82 mas (b, g), 87 mas (c, h), 87 mas (d, i), and 75 mas (e, j). In all figures the filter wavelength, the epoch of the observation, and the photometric phase  $\Phi$  are indicated. **k:** Cuts through the images a to e along the axis from component A to B (position angle  $20^\circ$ ).

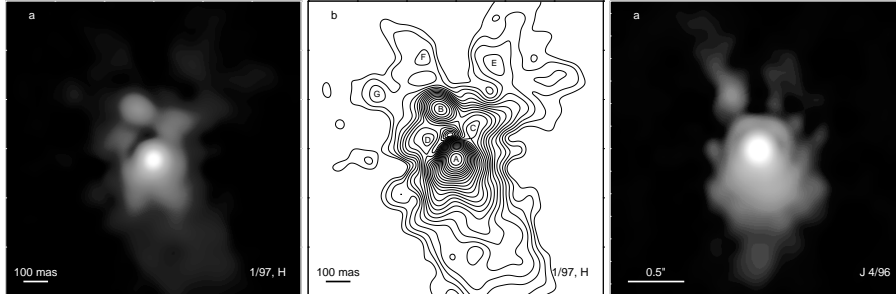


*Figure 2* **a**: 70 mas resolution bispectrum speckle interferometry image of IRC +10 216 in the *H*-band. North is up and east to the left. **b**: Same as (a) as a contour image with denotations (A to G) of compact structures. Contours are at every 0.2 mag down to 5.0 mag relative to the peak. **c** *J*-band speckle reconstruction of IRC +10 216 with 149 mas resolution.

ages from five epochs between Oct. 1995 and Nov. 1998 shows the dynamical evolution of the inner nebula (Fig. 1). Denoting the brightest four components with A to D in order of decreasing brightness in the 1996 image, the separation of the two brightest components A and B increased from 191 mas in 1995 to 265 mas in 1998, i.e. by  $\sim 35\%$ , corresponding to a relative velocity of 23 mas/yr or 14 km/s within the plane of the sky at  $d = 130$  pc. Within these 3 years the rather faint components C and D became brighter whereas component B faded. Note that the observations cover more than one pulsational cycle. Accordingly the apparent relative motions are not simply related to stellar variability. The general geometry of the nebula seems to be bipolar, most prominently present in the *J*-band image (Fig. 2) implying an asymmetric mass-loss.

The structures and changes in the inner nebula lead to the conclusion that the central star is close to or at the position of component B. Correspondingly, the initially brightest component A is the southern lobe of a bipolar structure. Then, the star is strongly but not totally obscured at *H* and *K*. Consistently, component B is very red in the *H* – *K* color while A and the northern *J*-band components are relatively blue. This is supported by  $1.1 \mu\text{m}$  archival HST polarimetry data (April 1997; see Osterbart et al. 2000). The polarization pattern is predominantly centro-symmetric with its center close to component B, whereas it shows strong polarization in the northern arms and a still significant polarization at component A. Finally, detailed two-dimensional radiative transfer calculations (Men’shchikov et al. 2000; this volume) show that the observed intensity ratio of A to B as well as the components’ shapes clearly require the star to be at B. The inner nebula and the apparent motions seem to be rather symmetric around this position and the observed changes suggest an enhanced mass loss since 1997. A strongly variable mass loss operating on timescales of

several stellar pulsation periods has, in fact, been predicted by dust-formation models of long-period carbon stars (Winters et al. 1995; this volume).

IRC+10216 is without doubt in a very advanced stage of its AGB evolution. The observed bipolarity of its dust shell even indicates that it has possibly entered the phase of transformation into a protoplanetary nebula.

### 3. H-DEFICIENT POST-AGB STARS

The most likely scenarios invoked to explain the H-deficient WR central stars are related to thermal pulses occurring either at the very end of the AGB evolution or during the post-AGB stage. During thermal pulses, recurrent instabilities of the He-burning shell, the luminosity of the He shell increases rapidly for a short time of 100 yr to  $10^6 \dots 10^8 L_{\odot}$ . The huge amount of energy produced forces the development of a pulse-driven convection zone which mixes products of He burning, i.e. carbon and oxygen, into the intershell region. Because the hydrogen shell is pushed concomitantly into cooler domains, hydrogen burning ceases temporarily allowing the envelope convection to proceed downwards after the pulse, to penetrate those intershell regions formerly enriched with carbon (and oxygen), and to mix this material to the surface (3<sup>rd</sup> dredge up). After the pulse hydrogen burning re-ignites and provides again the main source of energy (see Blöcker 1999 for a review).

Herwig et al. (1997) showed that the consideration of diffusive overshoot (Freytag et al. 1996) in all convective boundaries leads to important changes in AGB models, i.e. to (i) efficient dredge-up and formation of low-mass carbon stars; (ii) formation of  $^{13}\text{C}$  as a neutron source to drive the *s*-process in these stars; and (iii) considerably changed intershell abundances. The overshoot efficiency was calibrated by the observed width of the main sequence. The latter finding (iii) turned out to be a key ingredient for the modelling of WR central stars. Overshoot leads to an enlargement of the pulse-driven convection zone and to enhanced mixing of core material from deep layers below the He shell to the intershell zone resulting in intershell abundances (mass fractions) of (He,C,O)=(40,40,16) instead of (70,25,2) as in non-overshoot sequences. These modified intershell abundances are already close to the observed surface abundances of Wolf-Rayet central stars. Finally, in contrast to standard evolutionary calculations, overshoot models do show dredge up for very low envelope masses and efficient dredge up was found even during the post-AGB stage (Blöcker 2000, Herwig 2000) leading to the mixture of the intershell abundances to the surface and to the dilution of hydrogen. Three thermal pulse scenarios for Wolf-Rayet central stars can now be distinguished:

**AGB Final Thermal Pulse (AFTP)**, occurring immediately before the star moves off the AGB. In this case the envelope mass is already very small ( $\sim 10^{-2}M_{\odot}$ ). During dredge-up a substantial fraction of the intershell re-

gion is mixed with the tiny envelope leading to the dilution of hydrogen and enrichment with carbon and oxygen. The resulting surface abundances depend on the actual envelope mass at which the AFTP occurs. For instance, Herwig (2000) found for  $M_{\text{env}} = 4 \cdot 10^{-3} M_{\odot}$  (H,He,C,O)=(17,33,32,15) after an AFTP. The AFTP leads to a relatively high hydrogen abundance ( $\gtrsim 15\%$ ) and predicts small kinematical ages for the PNe of WR central stars which emerge here directly from the AGB.

**Late Thermal Pulse (LTP)**, occurring when the model evolves with roughly constant luminosity from the AGB towards the white dwarf domain. This kind of thermal pulse is similar to the one experienced by AGB stars but the envelope mass is even smaller than for the AFTP ( $\sim 10^{-4} M_{\odot}$ ). Fig. 3 shows the evolutionary track of a  $0.625 M_{\odot}$  LTP model with diffusive overshoot (Blöcker 2000). After the flash the intershell abundances amounted to (He,C,O)=(45,40,13) and the model evolves towards the AGB domain. At minimum effective temperature ( $\approx 6700$  K) dredge up sets in and continues until the star has reheated to  $\approx 12000$  K. Hydrogen is diluted to 3% and the final surface abundances of He, C and O are close to those of the intershell region, viz. (45,38,12). Extension of convective regions and abundances are illustrated in Fig. 4 as function of age and effective temperature, resp. The kinematical age of the PN amount to a few thousand years .

**Very Late Thermal Pulse (VLTP)**, occurring when the model is already on the white dwarf cooling track, i.e. after the cessation of H burning. Then, the pulse-driven convection zone can reach and penetrate the H-rich envelope and protons are ingested into the hot, carbon-rich intershell region raising a H flash (Iben & McDonald 1995). The energy released by this flash leads to a splitting of the convection into an upper zone powered by H burning and a lower one powered by He burning. The upper convection zone is, however, short-lived because the available hydrogen in the envelope is quickly consumed. Finally, the star becomes hydrogen-free and exposes its intershell abundances at the surface. Herwig et al. (1999) found for a  $0.604 M_{\odot}$  overshoot model surface abundances of (He,C,O)=(38,36,17). The kinematical age of the PN is relatively high since the star has first to fade along the cooling branch down to a few  $100 L_{\odot}$  before the flash. For  $0.6 M_{\odot}$  one obtains typically  $t \gtrsim 20000$  yr.

All scenarios lead to hydrogen-deficient post-AGB stars with carbon and oxygen abundances as observed for Wolf-Rayet central stars. The variety of observations requires most likely all of these scenarios. Many objects have only very low hydrogen abundances, if any, favoring the LTP and VLTP. On the other hand, several Wolf-Rayet central stars are surrounded by young planetary nebulae (Tylenda 1996) and circumstellar shells (Waters et al. 1998) strengthening the AFTP and LTP. Within the current models roughly 20 to 25% of stars moving off the AGB can be expected to become hydrogen-deficient.

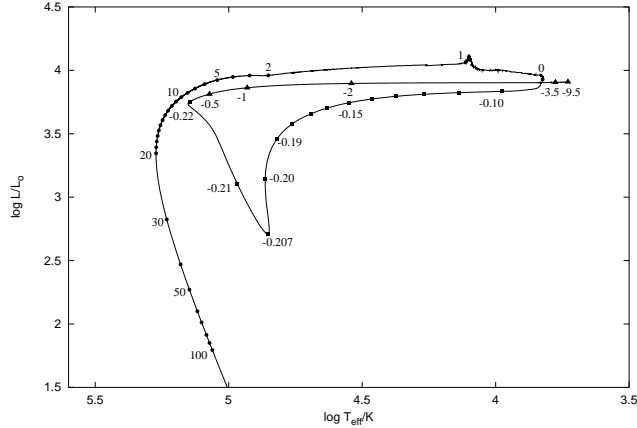


*Figure 3* Evolutionary track for a  $0.625 M_{\odot}$  overshoot model suffering from an LTP (Blöcker 2000). Symbols refer to time marks given in units of  $10^3$  yr. Time is set to zero at minimum effective temperature after the flash. The age -3500 yr marks the begin of the central-star evolution and refers to a pulsational period of 50 d. The preceding AGB evolution (Blöcker 1995) did not include overshoot. Since the intershell abundances of carbon and oxygen in overshoot AGB models first increase and then level out after a series of thermal pulses, they can be accounted for by calculating the pulse-driven convection zone with an enhanced overshoot efficiency ( $f=0.064$ ) leading to appropriate intershell abundances of  $(\text{He}, \text{C}, \text{O})=(45, 40, 13)$ . For the remaining evolution the standard efficiency ( $f=0.016$ ; Herwig et al. 1997) was used.

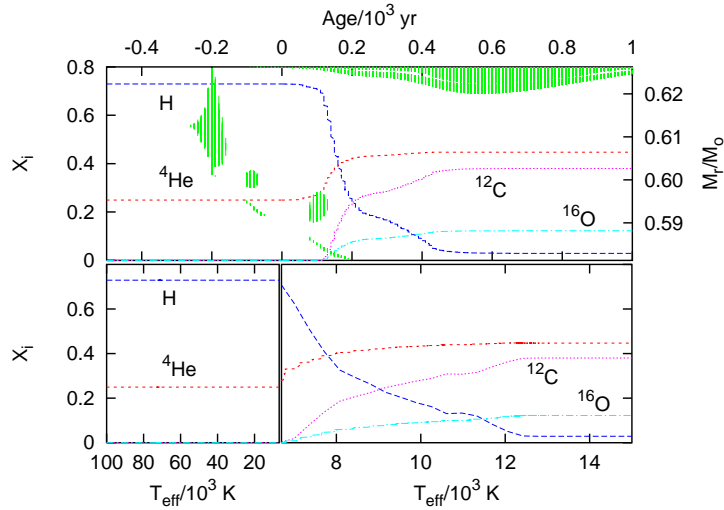


*Figure 4* **Top:** Evolution of the surface abundances of H, He, C, and O (left scale) and extension of convective regions (right scale) for the  $0.625 M_{\odot}$  overshoot model in Fig. 3 during flash and dredge up. Shaded regions denote convective regions. Time is set to zero at minimum effective temperature after the flash. **Bottom:** Surface abundances of H, He, C, and O as function of the effective temperature. The line indicates the turn-around point at minimum effective temperature after the flash corresponding to age zero in the above panel.

## References

- Blöcker T., 1995, A&A 299, 755.
- Blöcker T., 1999, AGB stars, IAU Symp. 191, T. Le Bertre, A. Lebre, C. Waelkens (eds.), p. 21
- Blöcker T., 2000, ApSS, in press
- Dreizler S., Heber U., 1998, A&A 334, 618.
- Dyck H.M., Benson J.A., Howell R.R., Joyce R., Leinert C., 1991, AJ 102, 200
- Freytag B., Ludwig H.-G., Steffen M. (1996), A&A 313, 497
- Groenewegen M.A.T., 1997, A&A 317, 503
- Haniff C.A., Buscher D.F., 1998, A&A 334, L5
- Herwig F., 2000, ApSS, in press
- Herwig F., Blöcker T., Schönberner D., El Eid, M., 1997, A&A 324, L81
- Herwig F., Blöcker T., Langer N., Driebe T., 1999, A&A 349, L5
- Iben I. Jr., MacDonald J., 1995, White dwarfs, Lecture Notes in Physics 443, D. Koester, K. Werner (eds.), Springer, p. 48.
- Kastner J.H., Weintraub D.A., 1994, ApJ 434, 719
- Koesterke L., Hamann W.R., 1997, A&A 320, 91.
- Kwok S., 2000, Asymmetrical Planetary Nebulae II, Kastner J.H., Soker N., Rappaport S.A. (eds.), ASP Conf. Ser. 199, p. 9
- Le Bertre T., 1992, A&AS 94, 377
- Lohmann A.W., Weigelt G., Wirtzner B., 1983, Appl. Opt. 22, 4028
- Loup C., Forveille T., Omont A., Paul J.F., 1993, A&AS 99, 291
- Mendez R.H., 1991, Evolution of Stars: The Photospheric Abundance Connection, IAU Symp. 145, G. Michaud, A. Tutokov (eds.), Kluwer, p. 375
- Men'shchikov A.B., Balega, Y., Blöcker T., Osterbart R., Weigelt G., 2000, A&A, submitted
- Olofsson H., 1996, ApSS 245, 169
- Osterbart R., Balega, Y., Blöcker T., Men'shchikov A.B., Weigelt G., 2000, A&A 357, 169
- Tuthill P.G., Monnier J.D., Danchi W.C., Lopez B., 2000, ApJ, in press
- Tylenda R., 1996, Hydrogen-deficient stars, C.S. Jefferey, U. Heber (eds.), ASP Conf. Ser. 96, 267.
- Waters L.B.F.M, Beintema D.A., Zijlstra A.A., de Koter A., Molster F.J., Bouwman J., de Jong T., Pottasch S.R., de Graauw T., 1998, A&A 331, L61.
- Weigelt G., 1977, Optics Commun. 21, 55
- Weigelt G., 1991, Progress in Optics 29, E. Wolf (ed.), North Holland, p. 293
- Weigelt G., Balega Y., Blöcker T., Fleischer A.J., Osterbart R., Winters J.M., 1998, A&A 333, L51
- Winters J.M., Fleischer A.J., Gauger A., Sedlmayr E., 1995, A&A 302, 483